Natural Fiber Suspensions in Thermoplastic Polymers. I. Analysis of Fiber Damage during Processing

Andrea Terenzi,[1] José M. Kenny,[1] Silvia E. Barbosa[2]

[1]*Materials Engineering Center, University of Perugia, Località Pentima Bassa, 21, 05100 Terni, Italy*
[2]*Planta Piloto de Ingeniería Química, PLAPIQUI (UNS-CONICET), Cno. La Carrindanga Km. 7, 8000 Bahía Banca, Argentina*

Received 22 February 2006; accepted 30 April 2006
DOI 10.1002/app.24704
Published online in Wiley InterScience (www.interscience.wiley.com).

ABSTRACT: The final properties of the composites materials are strongly dependent on the residual aspect ratio, orientation, and distribution of the fibers, which are determined by the processing conditions. Present work is a systematic study of the influence of natural fiber concentration on its damage during all the steps involved in the composite compounding. The system under study is cellulose fiber-reinforced polypropylene. The fiber geometrical parameters—length, diameter, and aspect ratio—are measured, and their statistical distributions are assessed for different concentrations. It is found that the higher the fiber concentration, the lower the fiber damage. These results evidence a difference in behavior between the damage of flexible natural fiber and rigid ones. The results are analyzed in terms of fiber concentration regimes, fiber–fiber interaction, flexibility, and entanglements. Two competitive mechanisms of the fiber interaction are proposed for explaining the fiber damage behavior during the flow of the flexible natural fiber suspensions. © 2006 Wiley Periodicals, Inc. J Appl Polym Sci 103: 2501–2506, 2007

Key words: natural fiber suspensions; fiber damage; cellulose–polypropylene composites

INTRODUCTION

Composites materials are currently used in many applications. Continuous thermosetting fiber composites are used mainly in applications with high technological contents such as aircraft and space industries because of their cost. On the other hand, short fiber thermoplastic matrix composites are used in other fields like automotive, sports articles, urban furniture helmets, etc. This fact is imputable to the use of commodity materials as matrix (with consequent cost reduction) and to the advantages in cost-effective processing and performance.[1]

The first reinforcements used, to increase the polymer rigidity, were glass, carbon, and aramid fibers. However, over the last years, many attempts have been made to replace the aforesaid fibers with others that satisfy requirements such as easy availability, low cost, good properties (when compared with traditional reinforcement), and low environmental impact. Natural fibers such as flax, cellulose, hemp, jute, sisal, etc., seem to offer a good response for these requirements. In fact, they are very cheap, available throughout the world, continuously renewable, and perfectly biodegradable.[2–9] These reinforcements also possess other advantages such as low density and good flexibility. The mechanical properties of natural fibers are comparable to that of the classical fillers such as glass, aramid, and carbon.[6] On the other hand, natural fibers are not abrasive, and this makes them very safe during the handling of the products, and moreover, they do not cause damage to the processing machine, resulting in low equipment wear during the composites manufacturing.[8,9]

Natural-reinforced composites are more recyclable compared with glass or carbon fiber-reinforced ones. The reduction in properties after recycling of natural composites is lower than that of the composites reinforced with rigid glass fiber.[5] Furthermore, the natural fibers are completely environment friendly: they are biodegradable and completely combustible; this is important when the plastic materials are incinerated for energy recovery.[8] On the other hand, natural fibers emit less CO_2, when they breakdown, than that is absorbed during plant growth.[10]

Currently, the main use of the natural fiber composites is for building materials such as tiles, doors, and windows. The most promising sector for these materials is the automotive industries.[10] These composites can be used for making of interior parts. Moreover, these materials can be used for making products like pottery, toys, and office objects.

Correspondence to: S. E. Barbosa (sbarbosa@plapiqui.edu.ar).
Contract grant sponsor: International Cooperation Project between Ministero degli Affari Esteri, Italy and Secretaria de Ciencia y Tecnologia, Argentine.

Journal of Applied Polymer Science, Vol. 103, 2501–2506 (2007)

The final properties of the composites materials are strongly dependent on the residual aspect ratio, orientation, and distribution of the fibers, which are determined by the processing conditions. During the manufacturing of short-fiber thermoplastic composites, they flow as suspensions of a polymer melt and short fibers. Then, the final fiber geometrical parameters depend on the fiber–fiber interaction and the interaction between fiber and the walls of the processing machine. The higher the fiber concentration, the higher the fiber interactions. However, the kind of the fiber–fiber interaction is different depending on their flexibility. Previous studies show that for glass fiber-reinforced polypropylene[11] compounded in a single screw extruder, higher fiber concentration leads to higher fiber damage. Also, they demonstrate that fiber length and the breath of this distribution decrease with extrusion rate. Czarnecki et al.[12] studied fiber damage and mastication characteristics of aramid-, glass-, and cellulose fiber-reinforced polystyrene melts, blending in an internal mixer. They found that glass fibers break down rapidly to very small aspect ratios, while aramid ones show a ''kinked'' structure. They also proposed a mechanism for fiber breakage based on buckling during rotation in shear flow. The results about cellulose fiber mastication are not very accurate because they say that the damage is least. No measures of geometrical parameters were done on cellulose fibers.

There are previous studies about fiber damage during processing.[2,13] They analyze mainly the effect of shear rate and temperature of manufacturing on final fiber length. However, the effect of fiber concentration on damage is not completely analyzed and understood. In the present work, a systematic and extensive study of the concentration influence on flexible natural fiber damage during manufacturing operations is performed. All fiber parameters—length, diameter, and aspect ratio—are taken into consideration in this analysis, correlating their variations to fiber–fiber interaction, concentration regime, and fiber flexibility. The results are interpreted in terms of concentration regime, fiber interactions, and fiber entanglements.

EXPERIMENTAL

Materials and compounding

Polypropylene *MOPLEN FL F20* in powder form (M_w: 240,000 g/mol; M_n: 94,000 g/mol), kindly supplied by Montell, was used as matrix. Natural fibers were obtained from sheets of cellulose pulp type LINCELL A, kindly supplied by Celesa. These sheets were reduced and separated by grinding in a high-speed rotational mill (Waring blender) at room temperature. After this, the fibers from cellulose pulp were well separated like fibers in cotton wools.

TABLE I
Name and Concentration of All Suspensions Prepared

Denomination	Fiber weight fraction ϕ	Fiber volume fraction ϕ_v
C0 (PP)	0	0
C10	0.10	0.069
C20	0.20	0.143
C30	0.30	0.222
C40	0.40	0.308

The fiber/matrix compounding was carried out in a batch mixer Haake Rheomix 90 at 190°C and 100 rpm. To improve the fiber dispersion, the mixer was fed with PP (powder) and ground cellulose pulp. The mixing was performed for 15 min to obtain a constant torque in the mixer. Samples with concentration of 10, 20, 30, and 40 wt % were prepared. Table I shows the characteristics of all samples prepared.

Several preliminary experiments were performed first to choose the method for mixing cellulose pulp with polymer to obtain a composite with fibers uniformly distributed. The first method included feeding the mixer with the polymer and cellulose pulp cut in small pieces, but the mixer was not able to homogenously disperse the fibers into the melt polymer. The second one included the dispersion of the fibers in water to enhance its separation, followed by a drying process and feeding the mixer with these fibers and the polymer. The problem was that, after drying, the cellulose fibers were agglomerated again, and the final dispersion was not very good.

Finally, the best final homogeneity in the composite was obtained by feeding the mixer with the ground pulp. In all the cases, the homogeneity control was primarily visual and, more accurately, using optical microscope.

Fiber characterization

Fiber density determination

The fiber density was measured according to the ASTM D 792 norm. This procedure is based on the Archimedes principle, and then, it depends on the weight of dry sample and the weight of the same sample immersed a fluid having a known specific weight. Ten samples were measured to statistically determine the specific weight of the cellulose pulp, and a value of 1.35 ± 0.04 g/cm^3 was obtained.

Fiber geometrical parameters

The fiber characterization was performed by transmission light optical microscopy studies using a Hund Wetzlar model H600 optical microscope. The images were acquired online and analyzed with Scion Image 4.0 software. Images with different magnifications

were acquired to accurately measure the fiber dimensions (length, diameter, and aspect ratio). The length of the fibers was assessed using low magnifications (2.5×) so as to have more complete fibers in each image. However, the diameter was measured on photographs with higher magnification for accuracy (10×). It is important to note that the measurement of flexible natural fiber is more complex than rigid ones. Flexible fibers had to be fitted with straight segments and the length is obtained as the sum of this. The amount of segment considered is a function of the fiber curvature.

The fiber dimension control was performed before and after the grinding (even before feeding) and after compounding in each concentration sample. In the first case, where the fibers are not mixed with the polymer, they were dispersed in water and put directly in a glass slide for microscope observations. In the second case, where fibers are into the composite, some small pieces of the composite were cut, melted, and compressed between two glass slides to obtain a thin film that can be observed in a transmission light microscope. With this method fibers are not damaged by any extracting process. More than 30 images were taken for each sample, and at least 150 fiber measurements were done to obtain the fiber length, diameter, and aspect ratio statistical distribution.

The distribution of the fibers geometrical parameters was assessed by calculating the probability density of the data. It was performed by the use of the expectation maximization algorithm (EM)[14] by means of MATLAB 5.3 program. This algorithm allows the assessment of the probability density function from a set of data (vector $x\ R^d$) using a linear combination of Gaussian functions. In this work, the Gaussian used proceeds form the class described by eq. (1).

$$p(x|\theta) = \sum_{i=1}^{n} \kappa_i N(x|\mu_i \Sigma_i) \tag{1}$$

where θ is a vector with components $(\kappa_i, \mu_i, \Sigma_i)_{i=1}^n$ subject to the following constrains applied are $\kappa_i \geq 0$ and $\sum_{i=1}^n \kappa_i = 1$. The term $N(x \mid \mu_i\ \Sigma_i)$ is the normal density (or Gaussian one) given by the eq. (2).

$$N(x|\mu_i \Sigma_i) = (2\pi)^{-d/2} |\Sigma_i|^{-1/2} \exp\left[-\frac{1}{2} \frac{(x-\mu_i)^i}{\Sigma(x-\mu_i)}\right] \tag{2}$$

The parameters in eqs. (1) and (2) can be calculated iteratively with the mentioned EM algorithm. The iterations are divided in two steps. The first one (step E) allows the estimation of the current parameters:

$$h_i^k = \frac{\kappa_i V(x^k|\mu_i \Sigma_i)}{\sum_{j=1}^n \kappa_j N(x|\mu_i \Sigma_i)} \tag{3}$$

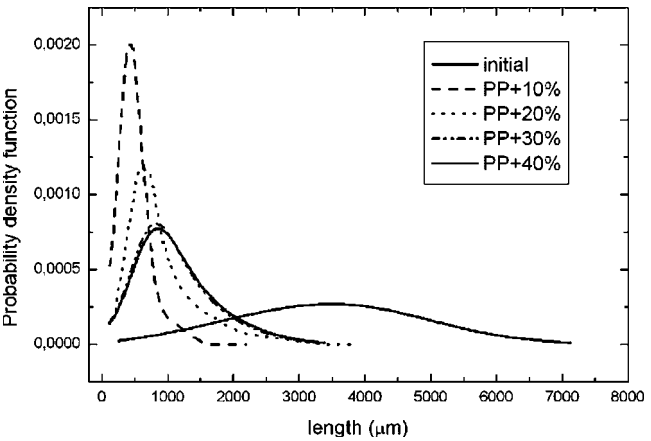

Figure 1 Fiber length distributions after compounding for all composites prepared.

The second step, called step M, permits to obtain the new parameters by

$$\kappa_i = \frac{1}{m} \sum_{k=1}^{m} h_i^k \tag{4}$$

$$\mu_i' = \frac{\sum_{k=1}^m h_i^k x^k}{\sum_{l=1}^m h_i^l} \tag{5}$$

$$\Sigma_i' = \frac{\sum_{k=1}^m h_i^k (x^k - \mu_i')(x^k - \mu_i')^T}{\sum_{l=1}^m h_i^l} \tag{6}$$

The values of the probability density for each set of data measured (length, diameter, and aspect ratio) were calculated by any iteration of this algorithm up to the convergence. Note that the present algorithm allows for the calculation of the probability density of each component of each input vector (length, diameter, or aspect ratio), but does not give the analytical expression of the distribution. Curves in Figures 1, 2, and 3 show the distribution for fiber diameter, length, and aspect ratio, respectively.

RESULTS AND DISCUSSION

Before compounding

Fiber dimensions suffer only a little change before compounding because of the grinding of the cellulose pulp. The average length, as well as the variance, changes around 4% from the initial ones, but the average diameter variation is one order of magnitude minor, 0.5%, as shown in Table II. These results are expected because the final dimensions of grinding pulp are much greater than the ''apparent'' single fiber length. Grinding is a mechanical effect more important

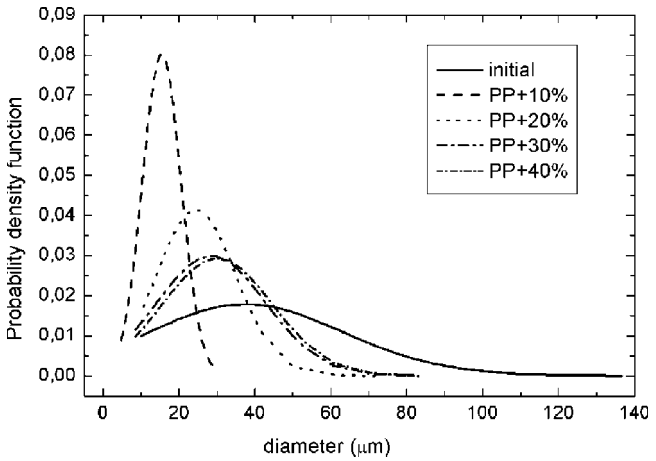

Figure 2 Fiber diameter distributions after compounding for all composites prepared.

for the length reduction than for fibrils separation. For understanding this, it is important to note that an ''apparent single fiber'' (from here called single fiber) is a group of single fibrils joined by lignin. Figure 4 shows a micrograph of the cross section of cellulose fiber. From this, it can be observed that each fibril is hollow and their walls are hollow too. The average diameter of a single fibril is around 1 μm, and not equal for all, and it depends on the wall thickness and the hollow dimensions.[15] Taking into account this fact, the two principal dimensions of the fibers change with grinding for cutting, detaching, and straining. The smallest fiber diameter reachable is the single fibril one. When the pulp is ground, the fibers are cut rather than they are detached, because the lignin joined is hard and increases the fiber toughness. The aspect ratio, as expected, decreases 4% because the length variation is greater than the diameter one. Figure 5 shows the optical microscopy images of the fibers after grinding. It is evident that the fibers are flexible and their diameter and length are not constant.

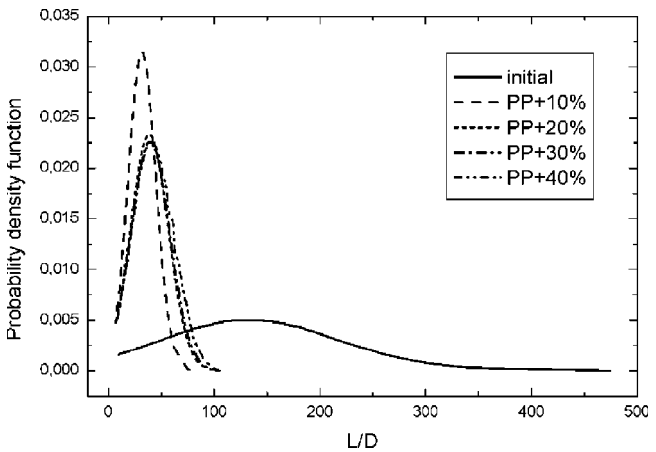

Figure 3 Fiber aspect ratio distributions after compounding for all composites prepared.

TABLE II
Average Values and Variance of Geometrical Parameters for Cellulose Fibers before Compounding

	Length L (μm)	Diameter D (μm)	Aspect ratio L/D
Before grinding	3448 ± 1451	37.1 ± 26.2	136.5 ± 86.5
After grinding	3297 ± 1261	36.9 ± 25.8	131.4 ± 82.3

After compounding

The variation in fiber geometrical parameters is more marked after compounding. Figures 1–3 show the fiber length, diameter, and aspect ratio distributions (area normalized) for all of composites prepared. Table III shows the average parameter values, and Figure 6 shows the average values normalized with its minimum as a function of fiber concentration.

The average length decreases 8.5 times for suspensions with 10 wt % of fibers, 7 times for those with 20 wt %, and around 6.5 times for higher concentrations. The lower the concentrations of fiber concentration suspensions, the narrower the fiber length distributions. It seems that from a critical concentration, the fibers suffer the same kind of damage. Note that the length distributions for 30 and 40 wt % match each other.

The fiber diameter distributions show a similar behavior as that of length distributions. However, the percentages of decrements are less than that for length, as it can be seen in Figure 6. Suspensions with 10 wt % of fibers suffer a decrement of 58% in the average diameter, while for 20 wt % of fibers, the diameter is reduced to 70% of the initial one and for 30 and 40 wt % to the 86%. Also for fiber diameter, the damage increases as the fiber concentration decreases.

The third parameter analyzed is the aspect ratio (L/D), the most important geometrical parameter in the determination of flow and final properties. Although it

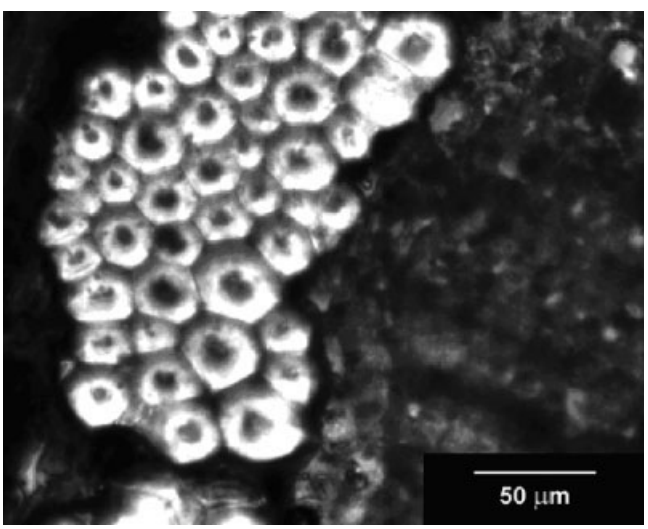

Figure 4 SEM micrograph of cellulose fiber internal structure.[15]

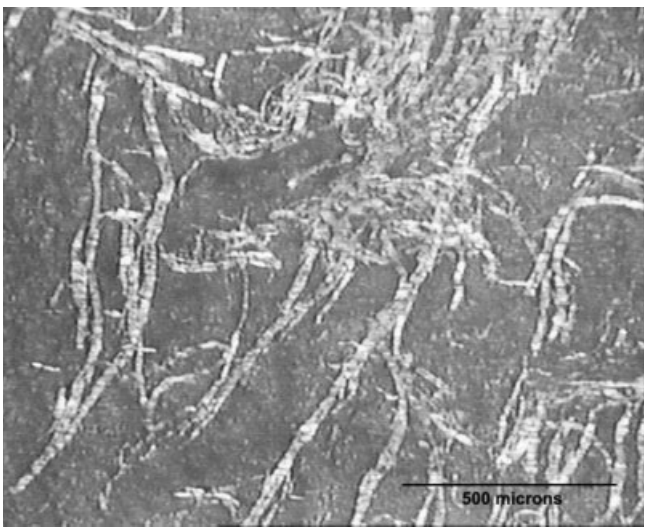

Figure 5 Optical micrograph of cellulose fiber before compounding and after grinding.

came from the relation between the length and the diameter, it shows different behavior with the concentration variation. For natural fibers, both fiber length and diameter vary after processing, whereas for glass fibers, the length varies but the diameter remains constant.[11,12] In the last suspensions, with higher fiber content, the fiber damage also increases. Usually, this performance is understood by taking into account the rigidity of the glass fiber. During the flow and processing, the two principal causes for fiber damage are the breaking due to fiber–fiber interaction and fiber attrition for friction with processing equipment walls.

The fiber length distribution for rigid fiber suspensions is similar to aspect ratio distribution, because the fiber diameter is constant. Nevertheless, for the natural fiber suspensions, the distributions get narrow as the fiber concentration increases; for 20 wt % of fiber content, the distribution matched perfectly and the average remained constant.

A first step in the comprehension of flow behavior is the determination of the concentration regime. Three typical regimes can be defined depending on the fiber–fiber interaction. When the fibers can move freely without encountering other fibers, the suspension is dilute. On the other hand, when fiber motion is restricted by others and cannot move, the suspension acts as a solid.

TABLE III
Average Values of Geometrical Parameters of Cellulose Fibers after Compounding

Name	Length L (μm)	Diameter D (μm)	Aspect ratio L/D
C10	484 ± 281	15.4 ± 5.1	31.6 ± 13.1
C20	977 ± 712	25.5 ± 10.5	38.5 ± 17.7
C30	1078 ± 631	28.51 ± 14.5	39.5 ± 18.4
C40	1116 ± 653	30.11 ± 14.6	40.1 ± 18.4

Between these two states, the fiber–fiber interaction occurs, and this is the semiconcentrated regime.[16] For rigid fibers, one suspension can be considered semiconcentrated if the fiber–fiber interdistance (h) is greater than its diameter and less than its length. Following the definition for average h given by Batchelor[17] for aligned fiber, the semiconcentration regime can be defined by the following expressions for random and uniform orientations, respectively:

$$\frac{1}{L^2} < n < \frac{1}{LD^2} \quad \text{or} \quad \frac{\pi}{4}\left(\frac{D}{L}\right)^2 < \phi_v < \frac{\pi}{4} \qquad (7)$$

The limits for the suspensions feed in the mixer are (average $L/D = 131$) $4.57\ 0.10^{-5} < \phi_v < 0.785$. The maximum packing volume fraction is 0.785. This maximum limit is valid also for flexible fibers, in the case that they are straight, tangent, and parallel to each other. According to this limit, all of the suspensions prepared (Table I) are semiconcentrated; they can flow, but fiber–fiber interaction is very important.

The typical parameters usually used for characterize rigid fiber suspensions with uniform fiber orientation gives the limits of fiber–fiber interactions; because they only take into account the fiber–fiber contacts, but not the flexible fiber entanglements. The interaction between flexible natural fibers is more complex than in the rigid ones because they buckle as demonstrated in Figure 7. There are two competitive interaction mechanisms that determine the final fiber dimensions. The first one is similar to the rigid fiber suspensions. The fibers hit each other and with the walls, and then they break.[18] On the other hand, because of the flexibility, they entangle generating a ''network.'' The higher the fiber content, the higher the fiber entanglements. Figure 7 corroborates it. The fiber network became denser, and therefore, this second mechanism controls the fiber interaction.

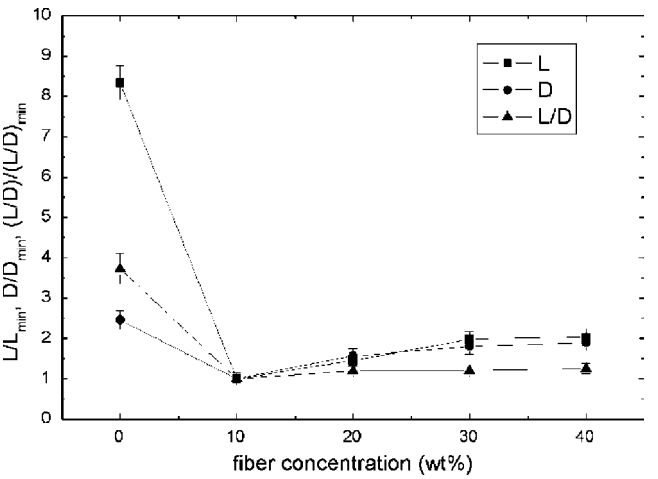

Figure 6 Fiber geometrical parameters normalized with the minimum value as a function of fiber concentration.

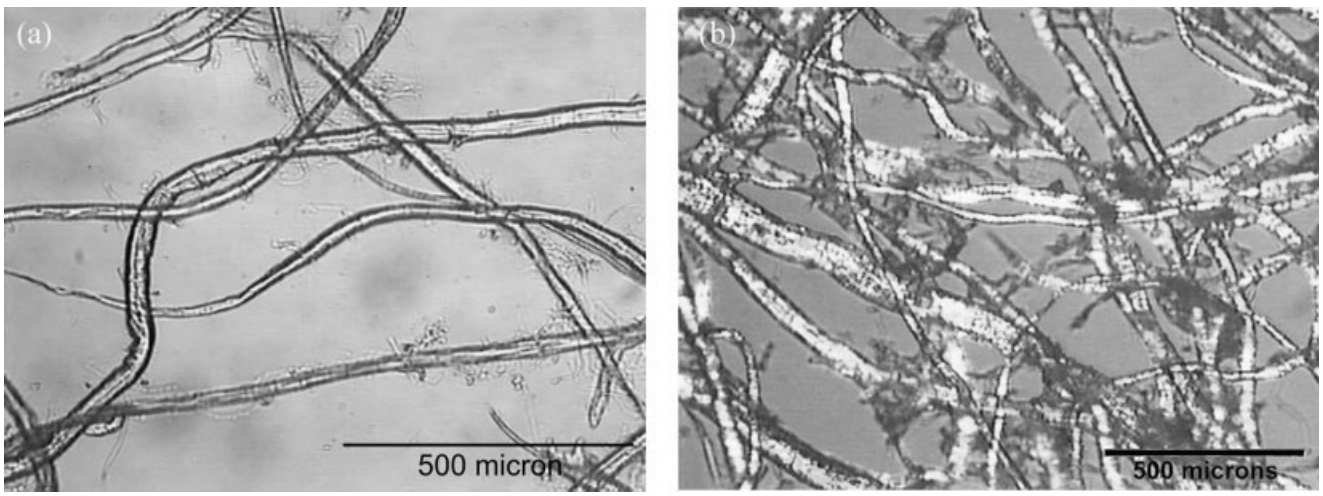

Figure 7 Optical micrographs of natural composite materials at different concentrations: (a) 10 wt %, (b) 30 wt %.

Based on this assumption, it is possible to understand the behavior of geometrical parameters with fiber contents. Actually, the first mechanism produces higher damage than the second one. In the last case, the fiber motion is so restricted by the others, and all the fibers in the network have an affine motion, and then, the attrition between them and against the walls decreases considerably.

The results showed earlier agree with this discussion. The higher dimension reductions were observed for the lower concentrations. The match in the parameters values for higher concentration (30 and 40 wt %) can be also explained. The fibers motion restriction remains constant from a determined amount of entanglements. More entanglements neither increase the motion impediments nor the fiber breaking.

CONCLUSIONS

This article presents an accurate study of flexible fiber damage before and after compounding. From the results and the discussion presented, the following conclusions can be arrived.

- Before compounding (after grinding), the damage in the fibers is not so important, up to 4%.
- After compounding, the lower the fiber concentration, the higher the geometrical parameters reduction.

The results were interpreted in terms of the fiber–fiber interaction, taking into account the fiber contacts (as rigid fiber suspensions) and the fiber entanglements (as flexible network). At low fiber contents, it seems that the behavior is similar to rigid fiber suspensions. However, at high fiber contents, the entanglement dominates the flow behavior. A limit concentration value from which the damage remains constant was obtained. This behavior introduces the idea of considering the concentrated flexible fiber suspensions as a flexible fiber network intercalated in highly entangled polymer molecules.

The authors gratefully acknowledge Dr. Jerico Biaggiotti for the interesting discussions.

References

1. Hartness, T.; Husman, G.; Koenig, J.; Dyksterhouse, J. Compos A 2001, 32, 1155.
2. Joseph, P. V.; Joseph, K.; Thomas, S. Compos Sci Technol 1999, 59, 1625.
3. Baiardo, M.; Zini, E.; Standola, M. Compos A 2004, 35, 703.
4. Li, Y.; Mai, Y. W.; Ye, L. Compos Sci Technol 2000, 60, 2037.
5. Rowell, R. M.; Sanadi, A. R.; Caulfield, D. F.; Jacobsen, R. E. In Proceedings of the First International Conference on Lignocellulosics-Plastics Composites; Leao, A. L.; Carvalho, F. X.; Frollini, E., Eds.; Sao Paulo, Brazil, 1997.
6. Canchè-Escamilla, G.; Rodriguez-Lavida, J.; Cauich-Cupul, J. I.; Mendizàbal, E.; Puig, J. E.; Herrera-Franco, P. J. Compos A 2002, 33, 539.
7. George, J.; Janardhan, R.; Anand, J. S.; Bhagawan, S. S.; Thomas, S. Polymer 1996, 37, 5421.
8. Stamboulis, A.; Baille, C. A.; Peijs, T. Compos A 2001, 32, 1105.
9. Thwe, M. M.; Liao, K. Compos A 2002, 33, 43.
10. Marsh, G. Mater Today 2003, 4, 27.
11. Barbosa, S. E.; Kenny, J. M. Polym Eng Sci 2000, 40, 11.
12. Czarnecki, L.; White, J. L. J Appl Polym Sci 1980, 25, 1217.
13. Jayaraman, K. Compos Sci Technol 2003, 63, 367.
14. Ormoneit, D.; Tresp, V. IEEE Trans Neural Networks 1998, 9, 43.
15. Biagiotti, J.; Puglia, D.; Kenny, J. J Nat Fibers 2004, 37, 1.
16. Doi, M.; Edwards, S. F. The Theory of Polymer Dynamics; Oxford University Press: Oxford; 1986.
17. Batchelor, G. K. J Fluid Mech 1971, 46, 813.
18. Chu, P. In Handbook of Polypropylene and Polypropylene Composites; Karian, H., Ed.; Marcel Dekker: New York, 1999; Chapter 9.